BULLETIN OF THE POLISH ACADEMY OF SCIENCES
TECHNICAL SCIENCES, Vol. 72(2), 2024, Article number: e148612
DOI: 10.24425/bpasts.2024.148612

Attitude Control System for an Earth observation satellite

Janusz NARKIEWICZ*, Szabolcs GRÜNVALD, and Mateusz SOCHACKI

Faculty of Power and Aeronautical Engineering, Warsaw University of Technology, Nowowiejska 24, 00-665, Warsaw, Poland

Abstract. The objective of the research was to develop the Attitude Control System algorithm to be implemented in the Earth Observation Satellite System composed of leader-follower formation. The main task of the developed Attitude Control System is to execute attitude change manoeuvres required to point the axis of the image acquisition sensor to the fixed target on the Earth's surface, while the satellite is within the segment of an orbit, where image acquisition is possible. Otherwise, the satellite maintains a nadir orientation. The control strategy is realized by defining the high-level operational modes and control laws to manage the attitude control actuators: magnetorquers used for desaturation of the reaction wheels and reaction wheels used for agile attitude variation. A six-degree-of-freedom satellite model was used to verify whether the developed Attitude Control System based on PID controllers for actuators performs attitude control in line with the requirements of an Earth Observation System. The simulations done for a variety of combinations of orbital parameters and surface target positions proved that the designed Attitude Control System fulfils the mission requirements with sufficient accuracy This high-level architecture supplemented by a more detailed control system model allowed proving efficient functionalities performance.

Key words: attitude control; Earth observing system; guidance; low Earth orbit satellites.

1. INTRODUCTION

A flight of two or more satellites with an accurately controlled position relative to each other, performing the same high-level mission objective is defined as formation flying [1]. Compared to conventional monolithic satellite designs, the benefits of satellite formations are additional mission flexibility, redundancy, and better damage tolerance. The satellites in formation may realize missions that otherwise would not be feasible [2].

A formation flying satellite system is elaborated as the 'EOS-WUT Earth Observation System' concept [3]. The goal of the EOS-WUT Earth Observation System (Fig. 1) is to demonstrate the feasibility and efficiency of nanosatellite formations used for image acquisition in Earth Observation missions [4]. The objective of this formation of two satellites is to perform image acquisition of a selected target on the surface of the Earth. The first satellite acquires a low-resolution image. A surface target is then selected for high-resolution imagery to be registered by the second satellite flying in the formation.

The two satellites are capable of automatically controlling their attitudes.

The objective of this research was to develop the Attitude Control System for such satellite formation, profiting from the previous work of the research team related to modelling actuators and actuator control systems. This paper focuses on the development of higher-level control laws and Attitude Control System operational modes to fulfil the described mission profile incorporating the actuator models and actuator controllers.

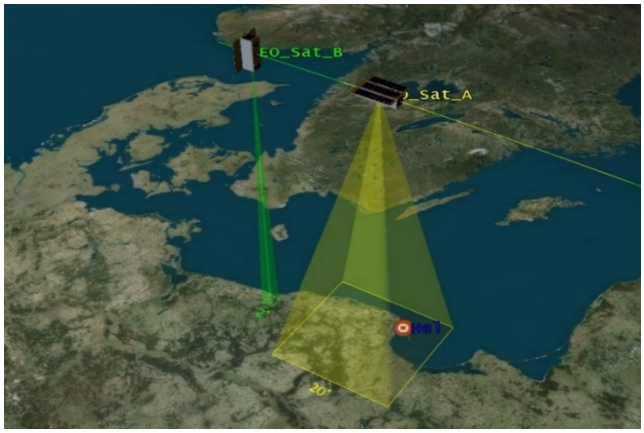

Fig. 1. Visualization of the two satellites in formation [4]

It is the main contribution to the field, allowing flexibility for system enhancement and adjustment to a specific spacecraft.

The remaining part of the paper is structured in the following order. First, the Attitude Control System requirements, operation, and structure are described, and the control laws are defined. Next, the simulation models of a satellite, sensors, and system are presented. A sample simulation results are finally presented, and conclusions summarize the main findings of the research.

2. SYSTEM REQUIREMENTS AND ARCHITECTURE

The main task of the Attitude Control System (ACS) is to manage actuator controllers according to the current and future orientation of the satellite relative to the inertial reference frame, which will allow effective image acquisition.

*e-mail: janusz.narkiewicz@pw.edu.pl

Manuscript submitted 2022-10-17, revised 2023-10-23, initially accepted for publication 2023-11-14, published in March 2024.

The length of a segment of a satellite orbit in which the image may be registered, named here "Image Acquisition Orbit Segment" (IAOS), depends on the field of view and the resolution of a satellite image sensors (Fig. 2). Within IAOS the axis of the image sensor points to the ground target. Otherwise, it points towards the nadir direction.

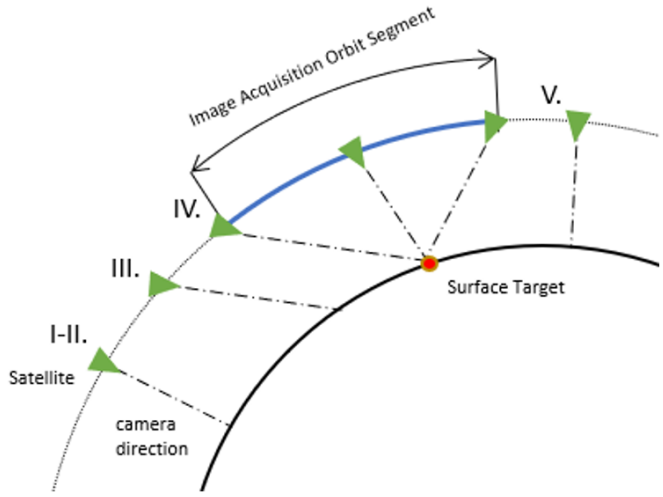

Fig. 2. Satellite attitude control during the image acquisition

The method of determining the IAOS is not considered in this paper.

Three modes of control system operation are considered depending on the position of the satellite in the orbit:

I. Until receiving the coordinates of the Earth surface target, the satellite imaging equipment points towards the nadir direction (standby mode).
II. After receiving the target coordinates, the satellite attitude is adjusted to the required orientation at the entry point of IAOS (arm mode).
III. Within the IAOS the satellite attitude is precisely controlled in order to point towards the surface target (acquisition mode).
IV. After leaving the IAOS the Attitude Control System again orients the imaging equipment towards the nadir direction (standby mode).

The spacecraft considered in this study is equipped with two types of actuators (Fig. 3):

- Reaction wheels for precision attitude control.
- Magnetorquers to desaturate the reaction wheels and to stabilize the satellite just after deployment in the orbit.

The orthogonal actuator configuration is used; the control axes of actuators are positioned along the three body frame axes, and one magnetorquer and one reaction wheel are placed along each axis (Fig. 3).

Two functionalities levels of the control system are defined:

I. The **Satellite Attitude Control**. This system control level defines the high-level control goals (the target attitude and target angular velocity of the satellite and enabling/disabling commands for the actuators) for the lower-level actuator control system based on the current and the required satellite states.

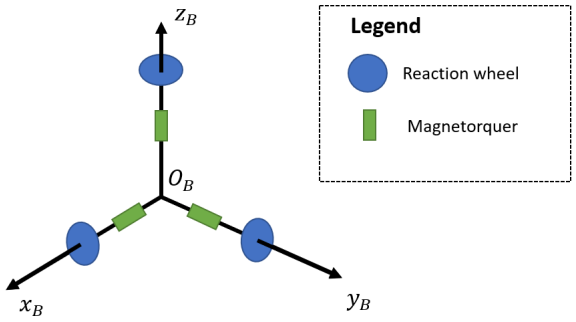

Fig. 3. Orthogonal configuration of actuators

II. The **Actuator Control**. This system control level operates the actuators according to the commands received from the Satellite Attitude Control level.

3. CONTROL LAWS

In this section, the system modes according to the description in Section 2 are explained.

3.1. Standby mode

The commanded attitude of a satellite is to orient the axis of the image sensor towards the nadir direction. In the standby mode, the following control modes can be set for the actuator control system:

Standby-Nominal mode: Only the reaction wheels are active, orienting the satellite image sensor axis towards the nadir direction.

Standby-Detumble mode: If the angular velocities of a satellite are higher than the assumed threshold (e.g. when the satellite is deployed from the launcher and is subject to tumbling), the magnetorquers are activated to suppress angular velocities below the threshold.

Standby-Desaturate mode: When the angular velocities of the reaction wheels are above the assumed threshold, the reaction wheels are decelerated until their angular velocity due to the rotational friction decreases below a safe value. The magnetorquers are activated to counteract the torques acting on the satellite due to the deceleration of the reaction wheels. Usually, the saturation thresholds of angular velocities of reaction wheels are assumed low enough to prevent the saturation of reaction wheels during the attitude change manoeuvres in the upcoming IAOS.

3.2. Arm mode

The satellite enters this mode to be ready for image acquisition at the entry of IAOS. The following conditions should be fulfilled to activate this mode:

- The detumbling process is completed.
- The angular velocities of the reaction wheels are below the saturation thresholds.
- The satellite is within an adequate distance (time) before entering IAOS.

The arm mode may also be activated after the acquisition mode if subsequent image acquisition is required of the surface target in a brief time.

The control task in the arm mode is to obtain the satellite attitude required to point towards the surface target at the entry to the upcoming IAOS. The control mode of the actuator control system is set to nominal; hence only the reaction wheels are enabled.

3.3. Acquisition mode

After completing the arm mode, the satellite enters an acquisition mode when it reaches the boundary of IAOS.

The task of an acquisition mode is to control the satellite attitude in such a way that the image sensor axis is continuously pointing towards the surface target. The actuator control system is set to the nominal mode; hence only the reaction wheels are enabled.

After leaving IAOS, the satellite may return to the Arm mode if the subsequent image is required in the near future, or to the standby mode otherwise.

The following directions can be requested from the satellite using its operational modes:

- The nadir direction in the ACS Standby mode
- The attitude required at the entry into IAOS
- The acquisition direction (towards the Surface Target) when the satellite is in the Acquisition mode

The main functions of the Attitude Control System are listed below:

1. Determining future image acquisition orbit segments
   The boundaries of the Image Acquisition Orbit Segments are calculated to allow the ACS to execute the manoeuvres of attitude change accurately and in time.
2. ACS control laws
   Using the defined control modes (Arm, Standby, Acquisition) the required attitudes (nadir or towards the surface target) and controls of the actuators (enable/disable the magnetorquers and reaction wheels independently) are calculated in this component.
3. Calculating error functions
   The attitude and angular velocities requested by the ACS control laws are calculated and the error between the current and requested attitudes and angular velocities is determined.
4. Magnetorquer controller
   When magnetorquers are enabled, this controller provides the control signals for the magnetorquers based on the difference between the current and the required angular velocities.
5. Reaction wheels controller
   When the reaction wheels are enabled, this controller provides the control signals for the reaction wheels based on the difference between the current and the required angular velocities and attitude angles.

4. SPACECRAFT MODEL

A six-degree-of-freedom satellite model was extended from the CubeSat Simulation Library in Simulink [5]. The spacecraft model is designed in a modular manner, hence allowing easily adding new functionalities, or removing non-essential components, so the satellite and system models can be quickly tailored to the requirements of research.

The core of the model is a six-degree-of-freedom satellite dynamic equation of motion in an ECEF (Earth-Centred Earth-Fixed) reference frame with a quaternion-based attitude [6] description and ellipsoidal WGS-84 Earth model. The satellite equations of motions are solved in the body fixed frame (BFF), which is fixed to the spacecraft centre of gravity here, and then the results are transformed to ECEF and ECI (Earth-Centred Inertial) frames. A location-dependent spherical harmonic gravity model [7] is used for calculating Earth's gravitational acceleration. The geomagnetic data is obtained from the MATLAB International Geomagnetic Reference Field model [8].

The reaction wheels (RW) are modelled as fixed-position flywheels in the satellite frame, driven by motors with controlled armature current [9] (Figs. 4 and 5, source: [10]).

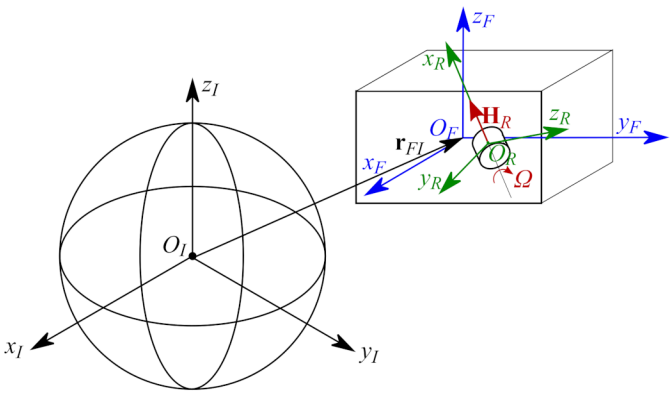

Fig. 4. Reaction wheel coordinate system [10]

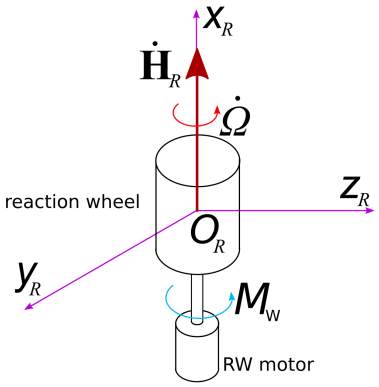

Fig. 5. Reaction wheel model [10]

A single RW angular momentum in the actuator coordinate system is calculated as:

$$\boldsymbol{H}_R = \begin{bmatrix} I_{Rx}(\Omega + \omega_{Rx}) & 0 & 0 \end{bmatrix}^T, \tag{1}$$

where:
$\boldsymbol{H}_R$ – angular momentum of the reaction wheel,
I_{Rx} – moment of inertia of the reaction wheel about its spin axis,

Ω – spin velocity of the wheel,
$\omega_R = \begin{bmatrix}\omega_{Rx} & \omega_{Ry} & \omega_{Rz}\end{bmatrix}^T$ – satellite angular velocity in the actuator coordinate system (Fig. 5).

The torque acting on the satellite due to a single reaction wheel (in the BFF frame) is calculated as:

$$\boldsymbol{M}_R = \begin{bmatrix} -I_{Rx}\left(\dot{\Omega}+\dot{\omega}_{Rx}\right) \\ -I_{Rx}\omega_{Rz}\left(\Omega+\omega_{Rx}\right) \\ I_{Rx}\omega_{Ry}\left(\Omega+\omega_{Rx}\right) \end{bmatrix}. \tag{2}$$

The angular velocity Ω is changed to vary the generated torque. The dynamics of rotation wheels are described by combined electromechanical equations; the armature current i_a is a direct control variable:

$$I_{Rx}\left(\dot{\Omega}+\dot{\omega}_{Rx}\right) = k_R i_R - b_R \Omega, \tag{3}$$

where: i_R – armature current, k_R – motor torque constant, b_R – viscous friction coefficient of the motor shaft.

The torque generated by a magnetorquer is a cross product of magnetic dipole generated by an actuator coil and the Earth's magnetic field:

$$\boldsymbol{M}_Q = \boldsymbol{D}_Q \times \boldsymbol{B}_Q = \begin{bmatrix} 0 & -D_Q B_{Qz} & D_Q B_{Qy} \end{bmatrix}^T, \tag{4}$$

where:
$\boldsymbol{D}_Q = \begin{bmatrix} D_Q & 0 & 0 \end{bmatrix}^T$ is a magnetic dipole generated by the coil,
$\boldsymbol{B}_Q = \begin{bmatrix} B_{Qx} & B_{Qy} & B_{Qz} \end{bmatrix}^T$ is a vector of the Earth's magnetic field in the magnetorquer coordinate system.

A magnetic dipole is calculated as:

$$D_Q = D_0 u_Q, \tag{5}$$

where D_0 – a nominal dipole moment of the magnetorquer at a given nominal voltage, u_Q – a control variable of a magnetorquer.

The satellite-commanded rotation is described by the vector:

$$\boldsymbol{y}_{cmd} = \begin{bmatrix} \boldsymbol{q}_{cmd} & \boldsymbol{\omega}_{cmd} \end{bmatrix}^T, \tag{6}$$

where
$\boldsymbol{q}_{cmd} = \begin{bmatrix} q_{0c} & q_{1c} & q_{2c} & q_{3c} \end{bmatrix}^T$ is the quaternion representation of the satellite-commanded attitude in the inertial frame,
$\boldsymbol{\omega}_{cmd}$ is the required angular velocity vector in the BFF coordinate system.

The required angular velocity $\boldsymbol{\omega}_{cmd}$ is calculated as [9]:

$$\boldsymbol{\omega}_{cmd} = 2 \cdot \boldsymbol{E}^T \cdot \dot{\boldsymbol{q}}_{cmd}, \tag{7}$$

where:

$$\boldsymbol{E} = \begin{bmatrix} -q_{1c} & -q_{2c} & -q_{3c} \\ q_{0c} & -q_{3c} & q_{2c} \\ q_{3c} & q_{0c} & -q_{1c} \\ -q_{2c} & q_{1c} & q_{0c} \end{bmatrix}. \tag{8}$$

The satellite attitude control vector is composed of control variables for the reaction wheels and magnetorquers:

$$\boldsymbol{u} = \begin{bmatrix} \boldsymbol{u}_R & \boldsymbol{u}_Q \end{bmatrix}^T, \tag{9}$$

where
$\boldsymbol{u}_R = \begin{bmatrix} u_{R1} & \dots & u_{RN_R} \end{bmatrix}^T$ contains the control variables for N_R number of reaction wheels,
$\boldsymbol{u}_Q = \begin{bmatrix} u_{Q1} & \dots & u_{QN_Q} \end{bmatrix}^T$ contains the control variables for t N_Q number of magnetorquers as defined above.

The inputs for the actuator controllers [9]:

- Current satellite rotation vector $\boldsymbol{y} = \begin{bmatrix} \boldsymbol{q} & \boldsymbol{\omega}_b \end{bmatrix}^T$.
- Required satellite rotational vector $\boldsymbol{y}_{cmd}$.
- Current angular velocity vector of the reaction wheels Ω.
- Required angular velocities of the reaction wheel Ω_{cmd}.

The PID controller was applied to control both actuators in the form:

$$\boldsymbol{u}_a = \alpha_P \cdot \boldsymbol{K}_p \cdot \boldsymbol{\sigma} + \alpha_D \cdot \boldsymbol{K}_D \cdot \boldsymbol{\omega}_e + \alpha_I \cdot \boldsymbol{K}_I \cdot \int \boldsymbol{\sigma}\, \mathrm{d}t, \tag{10}$$

where:
$\boldsymbol{\sigma}$ – difference between the required and current attitude,
$\boldsymbol{\omega}_e$ – angular velocity difference $\boldsymbol{\omega}_e = \boldsymbol{\omega}_{cmd} - \boldsymbol{\omega}_b$,
$\boldsymbol{K}_P$, $\boldsymbol{K}_D$, $\boldsymbol{K}_I$ – gain matrices for all control actuators,
α_P, α_I, α_D – parameters to more precise PID tuning.

The gain matrices are selected separately for the reaction wheels and magnetorquers.

The satellite attitude error is calculated as:

$$\boldsymbol{\sigma} = 2 \cdot q_{0e} \cdot \begin{bmatrix} q_{1e} & q_{2e} & q_{3e} \end{bmatrix}^T. \tag{11}$$

Quaternion $\boldsymbol{q}_e = \begin{bmatrix} q_{0e} & q_{1e} & q_{2e} & q_{3e} \end{bmatrix}^T$ is the attitude error quaternion calculated as [9]:

$$\boldsymbol{q}_e = \begin{bmatrix} q_{0c} & q_{1c} & q_{2c} & q_{3c} \\ -q_{1c} & q_{0c} & q_{3c} & -q_{2c} \\ -q_{2c} & -q_{3c} & q_{0c} & q_{1c} \\ -q_{3c} & q_{2c} & -q_{1c} & q_{0c} \end{bmatrix} \cdot \boldsymbol{q}, \tag{12}$$

and the angular velocity error is calculated as:

$$\boldsymbol{\omega}_e = \boldsymbol{\omega}_{cmd} - \boldsymbol{\omega}. \tag{13}$$

The expressions of the gain matrices for the reaction wheels were selected according to [9]:

$$\boldsymbol{K}_{PR} = \left(\omega_n^2 + \frac{2 \cdot \xi \cdot \omega_n}{T}\right) \cdot \boldsymbol{R}^{-1} \cdot \boldsymbol{G}_{RW}^{+} \cdot \boldsymbol{I}, \tag{14}$$

$$\boldsymbol{K}_{DR} = \left(2 \cdot \xi \cdot \omega_n + \frac{1}{T}\right) \cdot \boldsymbol{R}^{-1} \cdot \boldsymbol{G}_{RW}^{+} \cdot \boldsymbol{I}, \tag{15}$$

$$\boldsymbol{K}_{IR} = \frac{\omega_n^2}{T} \cdot \boldsymbol{R}^{-1} \cdot \boldsymbol{G}_{RW}^{+} \cdot \boldsymbol{I}, \tag{16}$$

where: $\boldsymbol{R} = \text{diag}\left(\begin{bmatrix} K_{t1} & \dots & K_{tN_R} \end{bmatrix}\right)$ – the diagonal matrix containing the reaction wheel motor constants, $\boldsymbol{G}_{RW}^{+}$ – the inverse or pseudoinverse of the matrix containing the direction of the axes of reaction wheels relative to the satellite body, ω_n – the control bandwidth, ξ – the dumbing ratio, T – the time constant of the controller, $\boldsymbol{I}$ – the satellite moment of inertia about its centre of mass.

Additionally, the sum of P-I-D components is saturated in the range of $[-1\ 1]$ to make sure that the $\boldsymbol{u}_{aR}$ signal is within its intended interval.

The proportional control was applied to magnetorquers:

$$\boldsymbol{u}_q = \boldsymbol{K}_{DQ} \cdot \boldsymbol{\omega}. \tag{17}$$

The $\boldsymbol{K}_{DQ}$ matrix depends on the location and time-dependent $\boldsymbol{B}_F$ magnetic field vector of Earth [9]:

$$\boldsymbol{K}_{DQ} = \boldsymbol{N}^{-1} \cdot \boldsymbol{G}_{MTQ}^{+} \cdot \frac{\boldsymbol{B}_F^x}{|\boldsymbol{B}_F|^2 \cdot \boldsymbol{K}_\omega}, \tag{18}$$

where: $\boldsymbol{G}_{MTQ}^{+}$ – the pseudoinverse or inverse of the $\boldsymbol{G}_{MTQ}$ matrix which contains the direction of the effective axis of individual magnetorquers, $\boldsymbol{B}_F^x$ – the skew-symmetric matrix of $\boldsymbol{B}_F$.

The value of $\boldsymbol{K}_\omega$ is calculated from the satellite moment of inertia matrix about its centre of mass $\boldsymbol{I}$, as $\boldsymbol{K}_\omega = \frac{4\pi}{T} \cdot \boldsymbol{I}$, the $\boldsymbol{N} = \text{diag}\left(D_{N1} \dots D_{nNQ}\right)$ diagonal matrix contains the D_{Ni} nominal dipole moments of the i-th magnetorquers, and the T orbital period of the satellite.

To decelerate the reaction wheels with a minimal impact on the satellite attitude the magnetorquers are enabled. The control of reaction wheels is set to zero.

5. SIMULATION OF SYSTEM OPERATIONS

The effectiveness of the Attitude Control System was verified by simulations. Two steps of simulation were done. First, the effectiveness of the isolated actuators was verified. In the second part, the system operation was simulated.

5.1. Efficiency of magnetorquers

The data used in this part of the simulations are given in Table 1 – Satellite orbit, Table 2 – Satellite and actuators, and Table 3 – Additional parameters. After code testing and debugging, the operation of actuators was simulated to check their ability to change the satellite attitude and to tune their controllers.

Table 1
Satellite orbital parameters

Parameter	Value
h satellite angular momentum	$6 \cdot 10^{10}$ m^2/s
e satellite eccentricity	0.2
i satellite inclination	0.5 rad
ω_o argument of periapsis	1 rad
Ω_o right ascension of the ascending node	0 rad
θ_0 satellite initial true anomaly at $t = 0$	3 rad

Table 2
Satellite and system data

Parameter	Value
Satellite mass	7.1 kg
Ixx inertia at the centre of mass	0.1614 kgm^2
Iyy inertia at the centre of mass	0.1854 kgm^2
Izz inertia at the centre of mass	0.1397 kgm^2
Magnetorquer type	NewSpace NCTR-M012 [11]
Magnetorquer dipole moment	1.19 A·m^2
Magnetorquer operational voltage	5 V
Reaction wheel type	Sinclair RW-0.03 [12]
Reaction wheel nominal moment	0.03 Nm
Reaction wheel moment of inertia about spin axis	51.16 kg·mm^2
Reaction wheel nominal voltage	6 V

Table 3
Additional parameters

Parameter	Value
Satellite NED Roll-Pitch-Yaw Euler angles	$[000]$ deg
Satellite ω_b body angular velocities relative to local NED	$[000]$ deg/s
Ground target Latitude-Longitude-Altitude (MSL)	$[000]$ deg, m

The detumbling mode was simulated for the initial satellite angular velocity in body axes: $\boldsymbol{\omega}_b = [10, 10, 10]^T$ deg/s, this scenario corresponds to the deployment of the satellite from the launcher. In the detumbling mode only magnetorquers contribute to the control moments. The angular velocities of the satellite in the body frame as functions of time are presented in Fig. 6. The satellite attitude was effectively stabilized after about five hours.

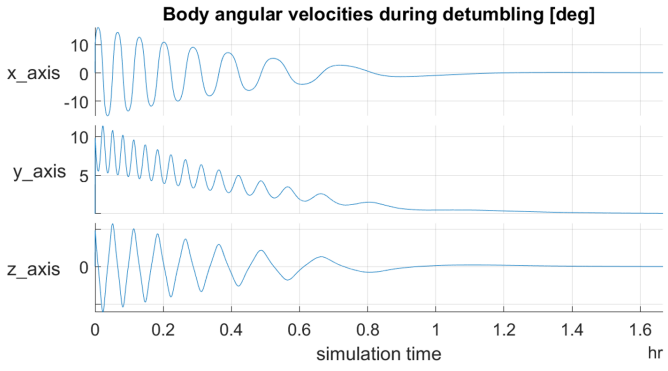

Fig. 6. Angular velocities during detumbling

5.2. Efficiency of reaction wheels

The objective of this test was to verify whether the reaction wheels model is correctly implemented, adequately tuned, and whether they can efficiently operate.

The required direction of the satellite sensor axis is first the nadir direction (as in the Nominal-Standby mode), then this direction is rotated by ±45 degrees about the sensor Oy axis (Fig. 7) with 100-second intervals between attitude changes. The tested attitude sequence is repeated as 1-2-1-3-1-2 based on the attitude states shown in Fig. 8.

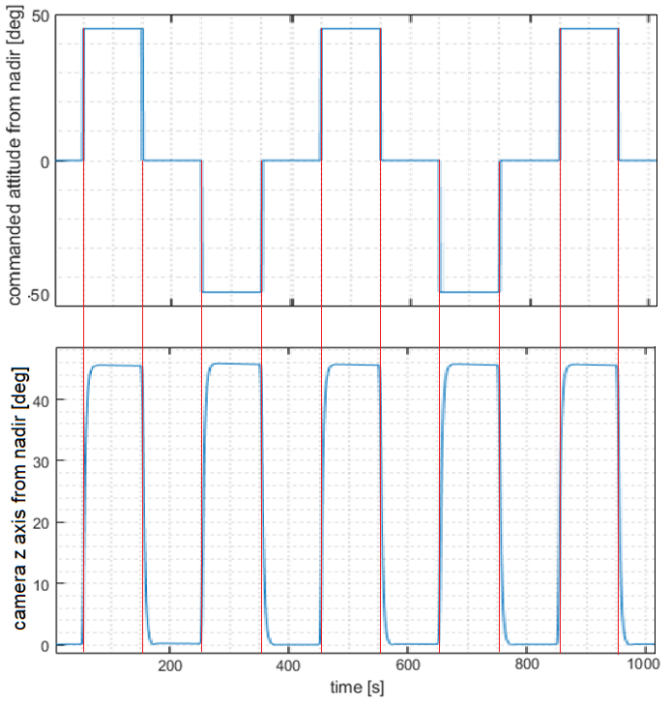

Fig. 7. Commanded and current camera angles from nadir during the reaction wheel test

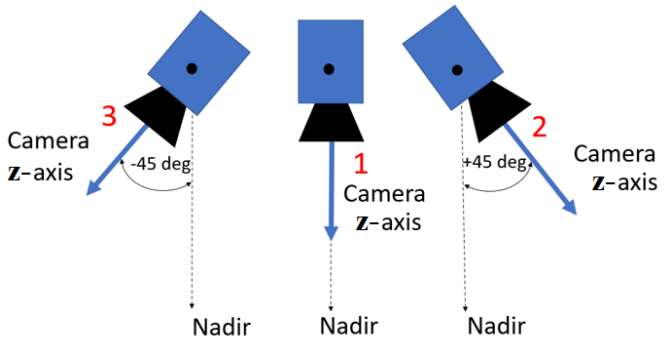

Fig. 8. Camera directions used for testing the operation of reaction wheels

The attitude commands (in terms of the angles between the camera Oz axis and the nadir direction) in function of time is plotted at the top part, and the angle between the camera Oz axis and the nadir direction is shown in the bottom part of Fig. 7. The time of commands to attitude changes (the rising and falling edges) are highlighted with red lines to facilitate easier comparison with the current angles, and to illustrate the controller efficiency during the multiple commands to change an attitude.

The commanded direction (Fig. 7) is only transient during the attitude change manoeuvres, outside of which the satellite attitude is stabilized, and the satellite attains the commanded attitude in a timely manner.

The attitude errors are illustrated for all axes of the satellite camera frame in Fig. 9, and the velocities in Fig. 10.

The angular velocities of the reaction wheels are presented in Fig. 11.

A close-up to attitude manoeuvre between 240–280 seconds is presented in Fig. 12.

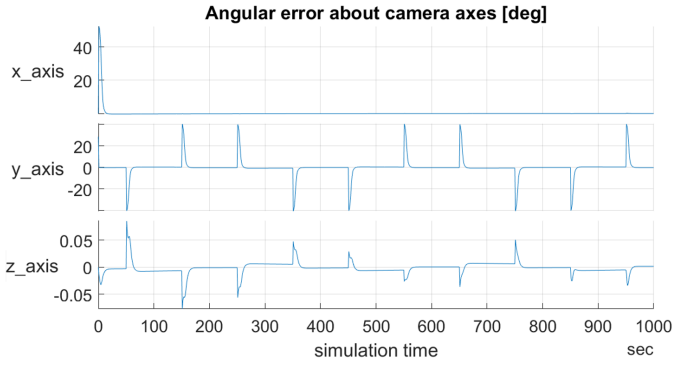

Fig. 9. Angular errors in the camera frame during the reaction wheel test

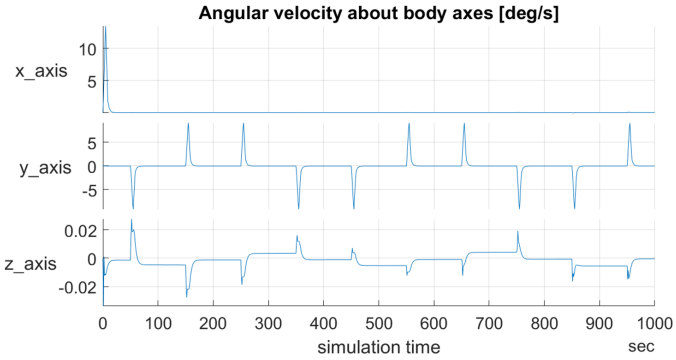

Fig. 10. Satellite angular velocities during test

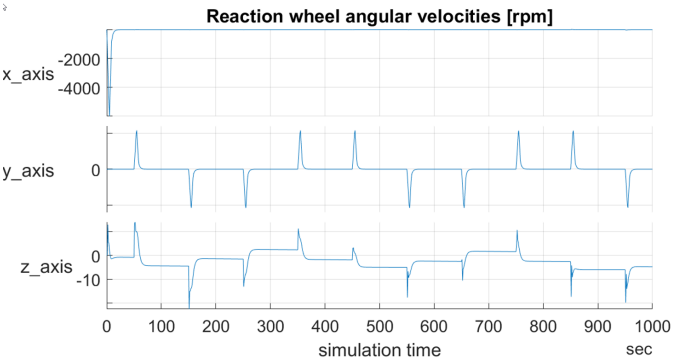

Fig. 11. Reaction wheel angular velocities during test

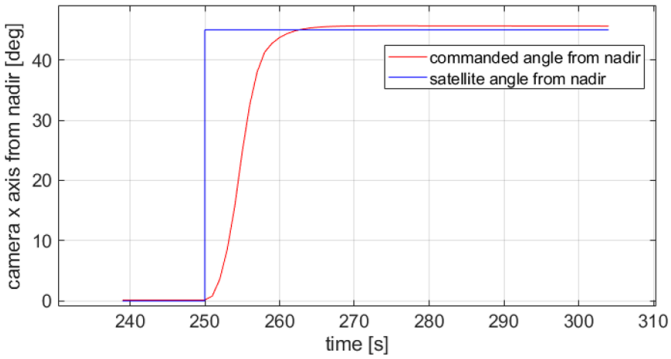

Fig. 12. Camera angle from nadir during the reaction wheel test

These and other simulations proved that the tuning of the PID controllers was adequate, and the reaction wheels were operating as required. The reaction of the satellite may be perceived as rather slow; however, it resulted mainly from the saturation of control inputs during the transient time. To counteract the slowness of the controller, the duration of the 'arm' mode of operational may be commanded adequately early, so the slow attitude variation would not affect the mission objectives.

5.3. System level test

The objective of this simulation was to evaluate the operation of the attitude control system for all modes. The following scenario was simulated (see Table 4):

1. At $t = 0$ the satellite has relatively high angular rates about all body axes; it imitates a deployment.
2. The detumbling process is performed, during which the satellite may enter the IAOS, but it remains in a detumbling process as its angular velocities are still too high.
3. When detumbling is completed, the control system switches to the standby-nominal mode.
4. Before reaching the IAOS boundary, the control system switches to the arm mode and changes its attitude to the required at the IAOS entry.
5. After entering the IAOS, the control system switches to the acquisition mode.
6. While in the acquisition mode, the satellite follows the surface target.
7. After leaving IAOS, the system returns to the standby-nominal mode.

The satellite and surface target parameters in this test that were modified are defined in Table 5.

Table 4
Operational modes during the system level test

Interval start	Interval end	Operational mode	Commanded camera axis direction
0 s	3209 s	Detumble	Nadir
3209 s	7246 s	Standby-Nominal	Nadir
7246 s	7312 s	Arm	Initial acquisition direction
7312 s	7703 s	Acquisition	Acquisition direction
7703 s	10000 s	Standby-Nominal	Nadir

Table 5
Modified satellite parameters for the system level test

Parameter	Value
h satellite angular momentum	$5.4 \cdot 10^{10}$ m^2/s
e satellite eccentricity	0.1
i satellite inclination	0 rad
ω_b satellite angular velocity in body axes at $t = 0$	$[10, 10, 10]^T$ deg/s
Ground target Latitude-Longitude-Altitude	[0 180 0] deg, deg, m
δ aperture of the acquisition cone	60 deg

The states set by the state machine during this simulation based on the analysed simulation results provide reference for the figures later:

Detumbling mode (0 s–3209 s): During the initial detumbling, the angular errors were oscillating as the satellite performed the detumbling process using magnetorquers only. After this manoeuvre was concluded, the satellite operated using the reaction wheels only, which resulted in significantly lower error margins.

Acquisition mode (7312 s–7703 s): It can be seen in Fig. 15 that when the satellite enters the Arm mode, it attains the attitude that will be required at the beginning of the Acquisition segment. The camera angle from the direction of the surface target decreases in an approximately linear manner in this mode, until it almost reaches 0 degrees just before entering the Acquisition mode at 7312 s. Then, when the satellite is in the Acquisition mode, the camera axis follows the direction of the surface target till 7703 s.

The angular errors for the entire simulation can be seen in Fig. 13.

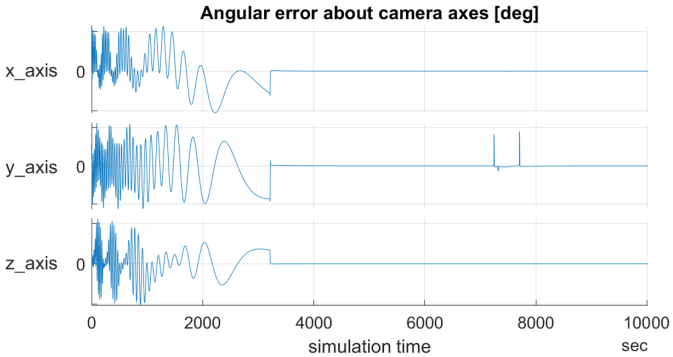

Fig. 13. Angular errors in the system level test

Standby-Nominal mode (3209 s–7246 s and 7703 s–10000 s): The angle between the camera axis and the nadir direction is presented in Fig. 14 to illustrate the efficiency of the controller in the nominal mode. The satellite follows the nadir direction well when commanded in the Standby-Nominal modes.

The results of this simulation illustrate that the satellite performs the required mission objectives with sufficient accuracy: when the satellite is within the acquisition segment, the mean

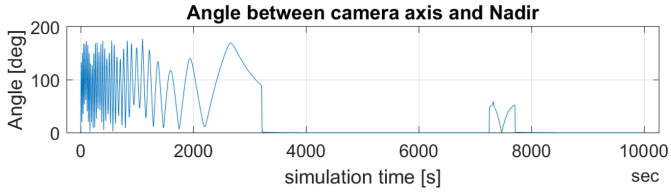

Fig. 14. Angle between camera axis and nadir direction for the system level test

error between the commanded and required attitudes is about 1 degree (Fig. 15) due to the rapidly changing direction of the surface target from the satellite position when the satellite is flying near it, and 0.05 degrees when the satellite is following the nadir direction commands (where the commanded direction does not change rapidly).

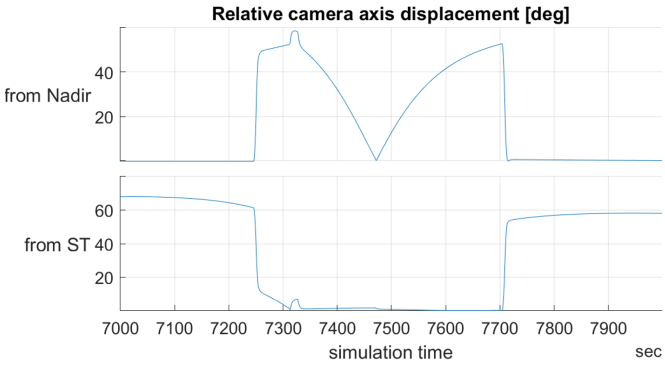

Fig. 15. Camera angles in Arm and Acquisition modes in the system-level test

The expected outcome of this simulation was that the satellite operational modes were set according to the required test scenario, and the attitude change manoeuvres were executed in an accurate and timely manner.

6. CONCLUSIONS

The Attitude Control System of a satellite was developed to perform the Earth Observation mission. High-level control laws and operational modes were defined to manage the attitudes of Earth Observation satellites using magnetorquers and reaction wheels. This high-level architecture supplemented by a more detailed control system model allowed to prove efficient functionalities performance.

When the satellite is within the orbital segment where acquiring the pre-selected ground target is possible, it is controlled to point its camera axis towards the ground target; otherwise, it is controlled to maintain camera axis points towards the nadir direction.

Two levels of control were defined. The high-level control laws are responsible for arbitrating between the control objectives and managing the actuators. The lower-level controls fulfil the control objectives (commanded directions) received from the higher-level controls, using PID-based algorithms.

A satellite model was established by customizing MATLAB's CubeSat Simulation Environment to be able to validate the developed Attitude Control System. The satellite model was expanded by the reaction wheel and magnetorquer models and controllers.

The developed Attitude Control System and its implementation in MATLAB were tested on both the component level and on the system level, proving its efficiency.

Further studies of the proposed Attitude Control System might include the examination of its robustness in the presence of external disturbances encountered at low Earth orbit environment (i.e. more detailed spatial distribution of the gravity field, solar radiation pressure, spacecraft-atmosphere interactions), as well as investigation of its limitations and potential control techniques.

REFERENCES

[1] S.D'Amico, "Autonomous Formation Flying in Low Earth Orbit," PhD thesis, Delft University of Technology, Netherlands, 2010. [Online]. Available: https://repository.tudelft.nl/islandora/object/uuid:a10e2d63-399d-48e5-884b-402e9a105c70/datastream/OBJ/download. [Accessed: 15. Nov. 2023].

[2] J. Soliz, "Formation flight of satellites around the Earth," in Proc. *Celestial Mechanics Seminar*, 2009, doi: 10.13140/ RG.2.2. 32038. 65603.

[3] J. Narkiewicz, S. Topczewski, and M. Sochacki, "A Concept of Nanosatellite Small Fleet for Earth Observation," presented at *4th Federated and Fractionated Satellite Systems Workshop*, Rome, Italy, 2016.

[4] D. Roszkowski, "Preliminary Design of Formation Flying Earth Observation System of Two Nanosatellites," B.Sc. Eng. thesis, Warsaw University of Technology, Poland, 2017.

[5] Mathworks, "Aerospace Blockset Cubesat library." [Online]. Available: https://www.mathworks.com/matlabcentral/fileexchange/70030-aerospace-blockset-cubesat-simulation-library. [Accessed: 15. Nov. 2023].

[6] Mathworks, "Aerospace Blockset 6DoF ECEF (Quaternion) block documentation." [Online]. Available: https://www.mathworks.com/help/aeroblks/6dofecefquaternion.html. [Accessed: 15. Nov. 2023].

[7] Mathworks, "Spherical Harmonic Gravity Model." [Online]. Available: https://www.mathworks.com/help/aeroblks/sphericalharmonicgravitymodel.html [Accessed: 15. Nov. 2023].

[8] Mathworks, "International Geomagnetic Reference Fieldle." [Online]. Available: https://www.mathworks.com/help/aeroblks/sphericalharmonicgravitymodel.html. [Accessed: 15. Nov. 2023].

[9] J. Narkiewicz, M. Sochacki, and B. Zakrzewski, "Generic Model of a Satellite Attitude Control System," *Int. J. Aerosp. Eng.*, vol. 2020, p. 5352019, Jul. 2020, doi: 10.1155/2020/5352019.

[10] B. Zakrzewski, "Satellite Attitude Control Using Magnetorquers and Reaction Wheels," M.Sc. Eng. thesis, Warsaw University of Technology, Poland, 2017.

[11] NewSpace Systems, "Magnetorquer rods catalogue datasheet (Version 8)." [Online]. Available: https://satcatalog.com/datasheet/NewSpaceSystems-NCTR-M012.pdf. [Accessed: 2. Mar. 2021]

[12] Sinclair Interplanetary, "Nanosatellite Reaction Wheels RW-0.03 datasheet Rev. 2019a." [Online]. Available: http://www.sinclairinterplanetary.com/reactionwheels/30 mNm-sec wheel 2019a.pdf?attredirects=0. [Accessed: 2. Mar. 2021]